ARTICLE

Dithiocarbamates as Capping Ligands for Water-Soluble Quantum Dots

Yanjie Zhang, Allison M. Schnoes, and Aaron R. Clapp*

Department of Chemical and Biological Engineering, Iowa State University, Ames, Iowa 50011-2230

ABSTRACT We investigated the suitability of dithiocarbamate (DTC) species as capping ligands for colloidal CdSe-ZnS quantum dots (QDs). DTC ligands are generated by reacting carbon disulfide (CS_2) with primary or secondary amines on appropriate precursor molecules. A biphasic exchange procedure efficiently replaces the existing hydrophobic capping ligands on the QD surface with the newly formed DTCs. The reaction conversion is conveniently monitored by UV−vis absorption spectroscopy. Due to their inherent water solubility and variety of side chain functional groups, we used several amino acids as precursors in this reaction/exchange procedure. The performance of DTC-ligands, as evaluated by the preservation of luminescence and colloidal stability, varied widely among amino precursors. For the best DTC-ligand and QD combinations, the quantum yield of the water-soluble QDs rivaled that of the original hydrophobic-capped QDs dispersed in organic solvents. The mean density of DTC-ligands per nanocrystal was estimated through a mass balance calculation which suggested nearly complete coverage of the available nanocrystal surface. The accessibility of the QD surface was evaluated by self-assembly of His-tagged dye-labeled proteins and peptides using fluorescence resonance energy transfer. DTC-capped QDs were also exposed to cell cultures to evaluate their stability and potential use for biological applications. In general, DTC-capped CdSe-ZnS QDs have many advantages over other water-soluble QD formulations and provide a flexible chemistry for controlling the QD surface functionalization. Despite previous literature reports of DTC-stabilized nanocrystals, this study is the first formal investigation of a biphasic exchange method for generating biocompatible core−shell QDs.

KEYWORDS: quantum dots • dithiocarbamate • FRET • biocompatible

INTRODUCTION

Luminescent quantum dots (QDs) are a relatively new class of fluorescent nanoparticles that possess exceptional photophysical properties, including strong resistance to photobleaching, broad excitation spectra, and narrow photoluminescence bandwidths. As a result, these nanoparticles have been applied broadly in fields ranging from clinical diagnostics (1−3) to photovoltaics (4, 5). A compelling aspect of QDs is the ability to precisely tune the emission spectrum by controlling the growth and composition of the nanocrystal. In developing a suitable QD for a particular application, the first consideration is choice of an appropriate semiconductor material with a bulk band gap energy that can be manipulated through the quantum confinement effect. As such, cadmium selenide (CdSe) QDs, despite their inherent toxicity concerns, are popular because of facile synthesis and tunable emission wavelengths that span most of the visible range. In many cases, a shell layer composed of a wider bandgap material than the core is desirable to contain the exciton and suppress non-fluorescent decay channels that sacrifice quantum yield (QY) (6). Core−shell QDs composed of CdSe-ZnS have been studied extensively and remain attractive for many applications requiring visible fluorescence.

Despite numerous significant advances in nanocrystal growth and preparation, QD behavior is often ultimately limited by the performance of the outermost ligands that bind the shell layer. These capping molecules are required to not only stabilize the nanocrystals in the preferred solvent, but they also provide critical electronic passivation to ensure that excitions decay primarily through a fluorescent pathway leading to the efficient emission of photons. In most cases, the choice of capping ligand is not nearly as important for organically soluble QDs as it is for QDs that are dispersed in aqueous media. This disparity is largely due to the tendency of polar media to introduce alternate routes of exciton relaxation that are non-radiative (7). In addition, various capping ligands may inadvertently introduce unfavorable HOMO-LUMO levels that compromise fluorescence emission; however, detailed analysis of this behavior is often difficult to assess in water using cyclic voltammetry. Further, the stability of these polar capping ligands is crucial to maintaining colloidal stability and suppressing these "dark" relaxation channels. In some cases, the stabilizing ligand is a vestigial product of the synthesis method and may not facilitate high quantum yield QDs.

A typical route for preparing water-soluble QDs is to perform a ligand exchange step after the initial crude product has been purified to remove excess precursors. There are many possible routes available; however, a common procedure is to precipitate the nanocrystals from solution and stir them in a neat or concentrated solution of the preferred ligand. Over time the hydrophilic ligands displace hydrophobic molecules at the nanocrystal surface such that the QDs are rendered water-soluble. Before the hydrophilic QDs can be used, they often require several cleaning stages (e.g., filtration or column chromatography) to remove displaced or excess ligands. To improve stability,

* Corresponding author. E-mail: clapp@iastate.edu. Phone: (515) 294-9514.
Received for review October 15, 2010 and accepted October 22, 2010

DOI: 10.1021/am100996g

Published on Web 11/05/2010

hydrophilic QDs are stored in a buffered solution at high concentration to avoid precipication due to desorption of the capping ligand from the nanocrystal surface. Even if QDs are soluble in water following the ligand exchange, the solution may only be stable for hours or days, which is impractical for most uses. Long-term stability of QDs in water requires a ligand that has a high affinity for the nanocrystal surface resulting in sufficient surface density to ensure solubility. This alone is a challenging goal; however, QDs also require ligands that passivate the surface defect sites, leading to bright, photostable nanocrystals.

The literature is replete with various methods for rendering QDs water-soluble (8−15). Many of these methods have focused on commercially available chemical species such as thiols which have reasonable affinity for a diverse set of nanoparticles including semiconductors and metals. A number of seminal studies (16, 17) focused on monothiolated molecules to stabilize QDs in water, and these ligands have been used continuously ever since. Unfortunately, unlike their behavior on gold nanoparticles, monothiols are generally not as stable on semiconductor nanocrystal surfaces (i.e., CdSe-ZnS) and are known to compromise (sometimes greatly) the luminescent quantum yield (18). Some improvements are observed by increasing the hydrocarbon chain length (for example, mercaptoundecanoic (19) versus mercaptoacetic acid (20)) to improve the hydrophobic interactions along the aliphatic chains and thus the protective nature of the capping ligands, but clearly monothiols have significant limitations because of the affinity of the single sulfhydryl group for the outermost shell layer of the QD. Although several groups (8, 21) have reported that the precise ligand exchange method used was critical to improving the stability and quantum yield using monothiols, the low binding energy between the monothiol and QD surface appears to be a significant limiting factor (2, 22), especially in aqueous buffers for biological applications (23). Recognizing the limitations of monothiol capping ligands, Mattoussi et al. (9) carefully investigated the use of lipoic acid (a bidentate thiol species) as a convenient ligand for solubilizing CdSe-ZnS QDs in water (based on a net negative charge in basic solutions) and forming stable conjugates with a recombinant protein having large net positive charge. The reduced form of lipoic acid, known commonly as dihydrolipoic acid (DHLA), has proved to be a stable ligand for long-term water solubility despite a lower density of ligands on the nanocrystal surface due to limits imposed by steric packing effects. The dithiol ligand has shown superior stability compared to monothiol ligands where QDs are routinely soluble in water for a year or even longer. However, DHLA is less beneficial in its role of preserving the luminescence properties of QDs. While some reduction in QY is common when transitioning QDs into an aqueous environment, thiolated ligands consistently reduce the QY far below that of the hydrophobic QD as prepared (e.g., QDs having alkyl phosphines in non-polar solvents). In the case of DHLA-capped QDs, the QY may vary significantly from one batch to another, however these water-soluble samples have fractional QYs in the range of 0.02 to 0.20. DHLA variants, such as DHLA conjugated to polyethylene glycol chains (DHLA-PEG) (24), display similar behavior to the parent ligand. Modifying DHLA via the terminal carboxy group is a useful platform for varying the functional group on a QD (25) and thus its behavior in solution; however, there appears to be no improvement to the QY over what is achieved with DHLA.

Focusing on methods that largely replace the native capping ligands on QDs with hydrophilic ligands, we examined the potential of dithiocarbamate (DTC) molecules to stabilize CdSe-ZnS QDs in aqueous media while maintaining high QY. Our work was motivated by the significant shortcomings of exsiting ligand-exchange procedures, which result in inferior water-soluble QD samples that are often inadequate for use in biological investigations for a variety of reasons: short-term stability, cell toxicity, poor luminescence, and pH instability. In addition to the need for long term colloidal stability and high QY, QDs used in biotechnology are required to sustain their properties over a wide range of pH and ionic strength. Further, our group has been especially interested in applying QDs to fluorescence resonance energy transfer (FRET) experiments where the overall size of the nanocrystal assembly is constrained by the scale of the calculated Förster distance (usually in the range of 4−8 nm). These requirements put severe restrictions on the types of capping ligands that may be used for practical applications, especially if the core-shell QD is relatively large. DTC species have been studied for many years as chelating ligands in synthetic chemistry and more recently as self-assembled surfactant molecules on gold surfaces and nanoparticles (26−28), but their history as capping ligands on QDs has been surprisingly limited, and nearly non-existent for core−shell QDs. To the best of our knowledge, this capping strategy has never been used with QDs for biotechological applications. The higher binding energy of the bidentate DTC to gold compared to monothiols as reported by von Wrochem et al. (29) suggests similarly high affinity of DTCs on semiconductor nanocrystals. Although there are have been intermittent reports of dithiocarbamate molecules functioning as QD capping ligands (28, 30−32), conclusions from these studies regarding their performance have been mixed which likely explains the limited use of DTCs as QD capping ligands generally. Moreover, given the diversity of ligands possible through a simple synthetic route and the lack of studies using core−shell QDs, it is clear that there has not been a thorough survey of dithiocarbamates as robust ligands for luminescent colloidal QDs, especially for biological applications.

Here we investigate the potential of DTC molecules to meet the broad challenges required of ligands for robust water-soluble CdSe-ZnS QDs which preserve their desirable optical properties. We are especially interested in comparisons of DTC-capped QDs with those bearing DHLA ligands (a ligand renowned for its stability) and the performance of these nanocrystals for FRET applications. Our approach is to consider a variety of primary and secondary amine-

containing molecules (those compatible with the DTC chemistry) and react these species with carbon disulfide to produce a candidate DTC ligand at high yield. Wherever possible, the reaction and cap exchange procedure is set up to take place simultaneously in a single reaction vessel where hydrophobic QDs suspended in an organic nonpolar phase are vigorously stirred with water and the hydrophilic amine in the polar phase (biphasic liquid mixture). Carbon disulfide (CS_2) reacts with the amino species to form a DTC molecule where the new ligand then chemisorbs onto the QD surface given sufficient time to transport from one phase to the other and bind the nanocrystal surface. Once complete, the process can be easily evaluated by noting the extent of QD transfer from the organic to aqueous phase. Ideally, QDs will fully transfer into the aqueous layer, where they preserve their fluorescence intensity. Candidate ligands for this study were chosen based on their commercial availability, reasonable cost, low molecular weight, solubility in water, and unique functional groups. The list of candidate ligands is virtually unlimited if we further consider custom synthetic molecules; however, this was not considered for this study. In some cases, a priori attractive candidate ligands performed poorly in our experiments, which highlights the need to conduct individual experiments rather than prematurely generalize about the prospects of a certain class of DTC-based ligands for this specific use. Given the numerous demands outlined previously for a robust water-soluble QD formulation, it seems likely that many promising potential ligands will fall well short of the demands placed on them. The results presented in this paper suggest that, despite this limitation, select DTC species are excellent QD ligands and that the diversity of potential ligands is vast and largely unexplored. Perhaps most appealing is the simplicity of the chemistry and post-reaction processing, which are accessible to virtually anyone with rudimentary chemistry laboratory experience.

EXPERIMENTAL METHODS

Materials. Hexadecylamine (HDA, 90%), hexamethyldisilathiane ($(TMS)_2S$), trioctyl phosphine (TOP, 90%), L-lysine (≥ 98%), and diethylzinc (Zn, 52.0 wt %) were purchased from Sigma-Aldrich and used as received. Cadmium acetylacetonate ($Cd(acac)_2$) and selenium shot (Se, 99.99%) were used as received from Strem Chemicals. Trioctyl phosphine oxide (TOPO, 98%) was obtained from Alfa Aesar and used as received. *n*-Hexylphosphonic acid (HPA) was purchased from Alfa Aesar and used as received. Aspartic acid (≥ 98%), L-cysteine (≥ 99%), L-histidine (98%), and L-threonine (98%) were purchased from Acros Organics and used as received. Chloroform and carbon disulfide (CS_2) were used as received from Fisher Scientific.

Methodology. ***(a) CdSe-ZnS Quantum Dot Synthesis.*** The quantum dots (QDs) used in this study, synthesized using the approach reported by Clapp et al. (33) and Howarth et al. (34) with some minor modifications, were CdSe-ZnS core–shell nanocrystals. Briefly, a three-neck flask containing TOP, TOPO, and HDA was degassed for three hours under deep vacuum and later backfilled with dry nitrogen gas (~3 psig) through a Schlenk line. Cd precursor ($Cd(acac)_2$) and Se precursor (1 M TOP:Se) were rapidly injected by syringe into the reaction chamber at high temperature (feedback-controlled heating mantle set at ~320 °C) with rapid mixing from a magnetic stir bar. The temperature was abruptly lowered (<100 °C) once the desired size had been reached as evaluated by UV–vis absorption. After annealing overnight (~80 °C), the CdSe cores were centrifuged for several minutes to remove excess reactants that accumulated at the bottom of the vial. To passivate and protect the cores from oxidation and the external environment, CdSe nanocrystals were overcoated with multiple ZnS layers (~3–5) to ensure a contiguous shell. CdSe core QDs were added to a fresh bath of ligands (TOPO and HPA), which was again degassed for 3 hours under a deep vacuum. Solvents used to store QD cores were evaporated and removed via a liquid nitrogen solvent trap before Zn and S precursors (diethylzinc and hexamethyldisilathiane, respectively) were added together dropwise at a rate of 0.4 mL/min using a programmable syringe pump. The resulting CdSe-ZnS core–shell QDs were again allowed to anneal overnight (~80 °C) and stored in a mixture of solvents (toluene, butanol, and hexanes to avoid freezing of excess ligands) for later processing.

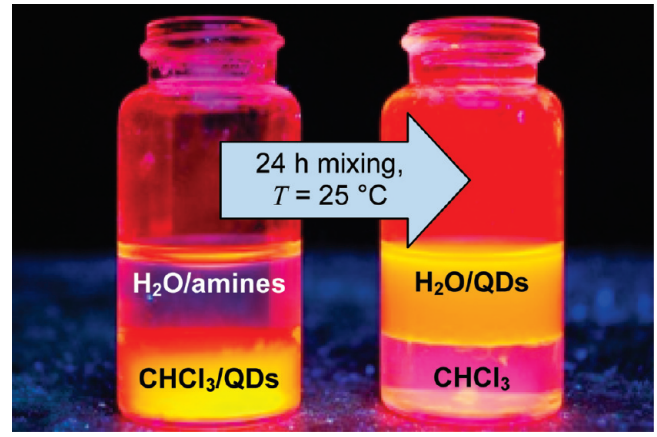

FIGURE 1. Transition of QDs from the organic to aqueous phase after stirring overnight in a capped glass vial. QDs from the organic layer (bottom) move into the aqueous buffer layer (top) following DTC-Lys reaction and ligand exchange.

(b) Biphasic Ligand Exchange. In a typical small-scale procedure suitable for a 20 mL glass scintillation vial, the synthesized CdSe-ZnS QDs described above were precipitated with dry methanol at least three times to remove excess hydrophobic ligands. The supernatant was discarded and the solid pellets (dried under N_2 flow) were dissolved in 5 mL of chloroform to a final concentration of 1.0 μM. 6.6×10^{-3} moles of the amino species (e.g., an amino acid such as lysine) was dissolved in 5 mL of ultrapurified water (or a suitable aqueous buffer) and 0.4 mL of CS_2 was added to the solution (the molar ratio of amino species to carbon disulfide is thus 1:1). When preparing a mixture of ligands, the total moles of both amino species should be 6.6×10^{-3} moles. Dithiocarbamate (DTC) species were formed immediately after agitating with a vortex mixer for 30 seconds and were monitored quantitatively by measuring its UV absorption spectrum (two distinct peaks: λ_{max} = 260, 290 nm) (26) at various time points during the reaction. The UV absorption spectra were measured by a Cary 50 Bio UV–vis spectrophotometer over a range of 200–800 nm using a 1 cm path length quartz cuvette. Both the QD solution and DTC solution were combined into a single 20 mL capped glass vial and vigorously stirred using a small magnetic stir bar for 24 h at room temperature although the process may reach completion in just a few hours. The next day, all QDs that were initially in the lower organic phase were observed in the upper aqueous phase indicating a successful reaction and exchange procedure. The process was further verified by exciting the sample with a handheld UV lamp (λ_{ex} = 365 nm) as Figure 1 shows. Excess reactants were removed by passing the resulting

sample through an Amicon Ultra-4 50k MW cutoff centrifugal filter (Millipore). The sample was (optionally) further cleaned by passing it through a PD-10 chromatography column (GE Healthcare). The processed samples were stored in either ultrapurified water (Milli-Q system, Millipore) or 1× phosphate buffered saline (PBS), however other buffers may be substituted depending on the specific capping ligands used and intended application. We found that the reaction and exchange procedure works well at the scale described above; however, we determined that it is possible to scale up the process substantially provided the larger reaction vessel allows adequate mixing.

(c) pH Sensitivity of Cap-Exchanged QDs. Following the cap exchange procedure and any additional cleaning steps, the fluorescence intensity of QDs coated with different DTC-ligands in varying pH was measured by a Fluoromax-4 dual monochromator spectrofluorimeter (Horiba Jobin-Yvon) with 0.1 s integration time. Spectra were corrected for dark noise and the wavelength-dependent quantum efficiency of the detector. Buffers of varying pH were prepared by adjusting the ratio of 0.2 M sodium phosphate to 0.1 M citric acid. DTC-capped QD stock solution was added to different aqueous buffers (from pH 3 to 7) to a final concentration of 40 nM for fluorescence measurements in a 0.4 cm path length quartz cuvette. For comparison, the stability of DHLA-capped QDs in different pH buffer solutions was also measured where all water-soluble QDs were prepared from the same hydrophobic stock QD solution.

(d) Cell Culturing and TIRF Microscopy. MDA-MB-231 breast cancer cells were purchased from ATCC and grown in Dulbecco's modified Eagle media (DMEM) with 4.5 g/L D-glucose, 1% sodium pyruvate, 1% L-glutamine, 10% fetal bovine serum (FBS), and 1% antibiotic pen/strep. Cells were incubated in DMEM with 0.15 μM DTC-Cys QDs and 10% FBS at 37 °C for 3 h. They were then washed with 1× PBS before being trypsinized. Fresh DMEM was added and followed by centrifuging at 1500 rpm for 5 minutes. After the supernatant was discarded, cells were plated onto a clean glass coverslip in growth media at a density of approximately 7×10^4 cells/mL and incubated at 37 °C for another hour before imaging. The coverslip was pre-coated with 0.03 mg/mL collagen to encourage adhesion of cells to the substrate. Imaging was performed using a Nikon Eclipse Ti-E inverted microscope fitted with a proprietary dynamic focus control system and fiber-based total internal reflection fluorescence (TIRF) illumination package. Excitation of the sample was achieved using a variable power diode laser system from Blue Sky Research ($\lambda_{em} = 442$ nm, 45 mW) which is ideal for producing fluorescence in any CdSe-ZnS QD sample while avoiding direct excitation of any organic dyes. Images were collected using a Nikon 60× TIRF objective (having a numerical aperture of 1.49) and a Photometrics CoolSNAP HQ^2 CCD camera using Micro-Manager open source software (release 1.3) and appropriate plug-ins. The exposure time was set to 400 ms with 5 second intervals between frames. Images were further processed and analyzed using NIH ImageJ software (release 1.43).

RESULTS AND DISCUSSION

DTC Formation and Ligand Exchange. Figure 2 shows the synthetic scheme for the production of DTC ligands and exchange onto QDs. The DTC ligands are able to displace the native hydrophobic groups (typically composed of varying ratios of TOP, TOPO, and HDA) populating the QD surface during biphasic exchange. The synthesis of DTCs was carried out by mixing carbon disulfide (CS_2) and amino precursor (containing at least one primary or secondary amine functional group) dissolved in ultrapure water. DTC ligands were formed immediately after the mixing CS_2 and amine precursor, the progress of which was monitored

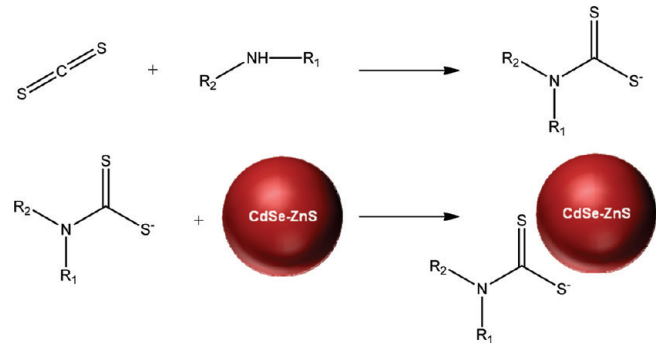

FIGURE 2. Chemistry and ligand-exchange scheme using DTC-derivatives on QDs.

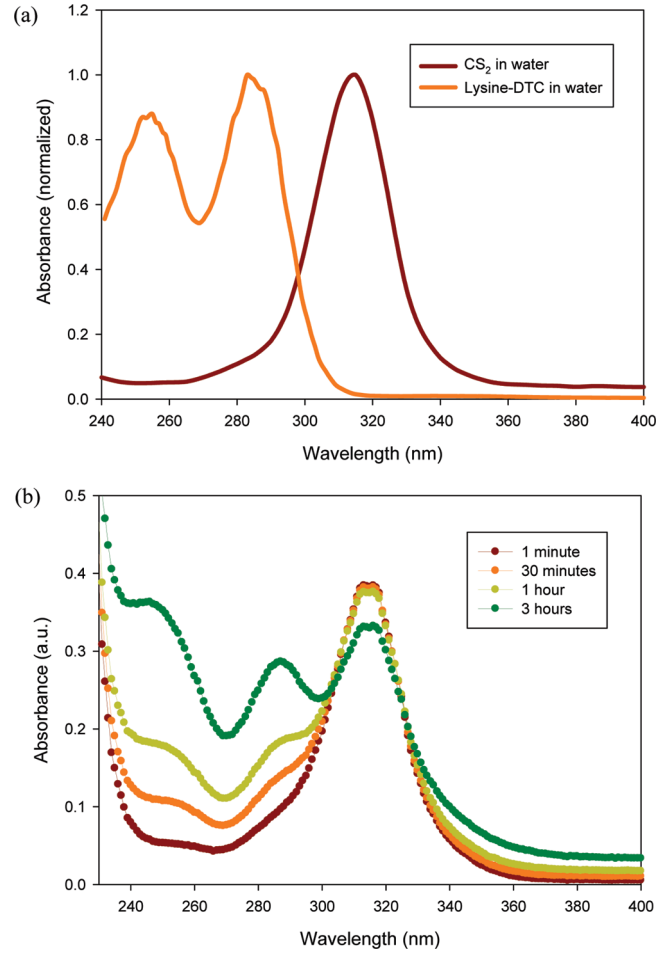

FIGURE 3. (a) UV absorption spectrum of DTC-Lys, formed in water. (b) UV absorption spectrum of DTC-Threonine, formed in water at various time periods.

via UV-vis absorption. DTCs have two characteristic UV absorption peaks: one at 260 nm and another at 290 nm, as shown in Figure 3a. Absorption spectroscopy is also a convenient way to evaluate the conversion of amino precursors to DTC ligands, especially if the reaction is slow or inefficient. Figure 3b shows a case where the reaction is slower than expected between CS_2 and the amino acid threonine (Thr). Here, the absorption peak of carbon disulfide ($\lambda_{max} = 315$ nm) persists while the peaks due to DTC formation increased only modestly after 3 h. It is apparent that Thr does not readily react with CS_2 to form a DTC species despite its high solubility in water and available

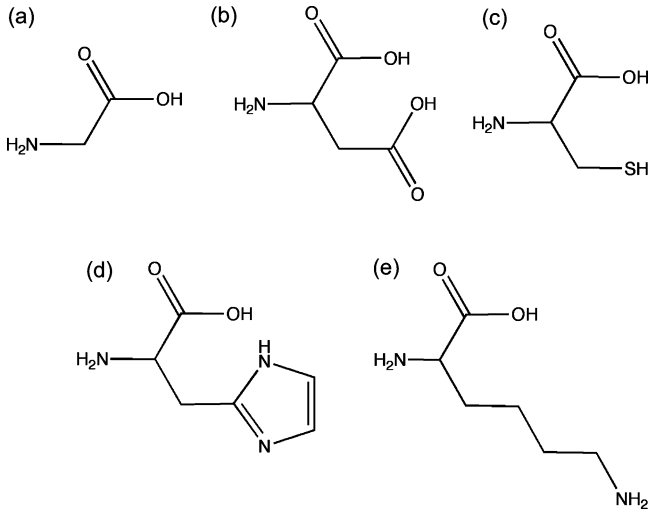

FIGURE 4. Chemical structure of amino acids used in this study: (a) glycine, (b) aspartic acid, (c) cysteine, (d) histidine, and (e) lysine.

primary amine. This is an example of a ligand that was an appealing prospect that did not behave as expected. In contrast, Figure 3a shows that the absorption feature from CS_2 completely disappeared, concomitant with a rise in the DTC peaks within 1 min, which demonstrates the speed and efficiency of this reaction under favorable circumstances (i.e., an appropriate amino species).

Amino acids were selected as candidate precursors in this study largely because they are biocompatible and commercially available, but also because of their low molecular weight, which minimizes the effective size of the resulting hydrophilic QDs. Their existing functional groups such as carboxyl (−COOH), thiol (−SH), amine ($-NH_2$), and imidazole ($-C_3H_4N_2$) allow QDs to directly conjugate to biomolecules by capping with a compact monolayer of ligands. We have investigated other potential ligand precursors as well, but because of the unique aspects of those results, we have restricted the present report to amino acids. The chemical structures and general properties of the amino acids used in this study are shown in Figure 4 and Table 1, respectively (35, 36). The solubility of a particular amino acid in water is a significant limiting factor in the synthesis of DTC ligands using this particular method because eventually this molecule is used to render QDs water-soluble. We found that some amino acids having relatively poor water solubility at neutral conditions, including histidine (His) and aspartic acid (Asp), were more soluble in basic solutions, while other amino acids such as glycine (Gly) and lysine (Lys) increased the pH to ∼10−11 once fully dissolved in water. In contrast, cysteine (Cys) was highly soluble in neutral aqueous solutions and found to react completely irrespective of the reaction conditions. Although water solubility of the amino species is a necessary criterion for the reaction and exchange to proceed efficiently, it is not always sufficient, as in the case of Thr, which is highly soluble in water but did not react completely with CS_2. Because of varying behavior in water, some combinations of amino acids functioned well together during the reaction and exchange process. For example, the overall solubility of His and Asp was substantially improved (over their individual solubility) by mixing equal molar amounts of the two amino acids together in solution where they could be converted into DTC ligands for a mixed-surface exchange. Another benefit of using mixed ligands is to provide QDs multiple functional groups where, for example, one type of amino acid primarily serves to solubilize the QDs in water while another provides QDs desirable function or affinity. The diversity of available ligands (beyond amino acids) suggests that many useful combinations are possible and requires further study depending on the intended application.

The ligand exchange is facilitated by choosing appropriate solvent(s) and mixing or agitating the sample thoroughly. For the two-phase process used in these experiments, we chose water and chloroform as the polar and non-polar solvent pair, respectively, which are effectively immiscible; the former is just under 1 % (w/w) soluble in the latter. We found that the biphasic exchange was far more efficient using chloroform as the organic phase than toluene, which has 20-fold lower solubility in water (∼0.05 % w/w). Other solvent combinations may result in efficient reaction and exchange, but were not examined in this study due to the initial effectiveness of chloroform. Vigorous mixing greatly enhances the contact area between two immiscible phases and is essential for an efficient ligand exchange process. Sonication of the sample may also be a suitable method for improving the exchange and could be used in place of or in conjunction with rapid stirring. In most cases the exchange showed evidence of reaching completion well before 24 h (usually in the range of 4−6 h). The speed of the exchange procedure can be individually assessed spectroscopically and through a long-term examination of colloidal stability. An exchange was deemed to be successful if the QD sample was sustained in water and moderately luminescent (apparent by eye) for more than a week. Many samples were stable for much longer periods (typically several months). We also discovered that freezing DTC-capped QDs at micromolar concentrations in water/buffer was an effective method for preserving their properties until the sample is needed. There were no deleterious effects of freezing water-soluble QD samples at −10 °C for several days or weeks, and presumably, this storage method could be used for much longer periods as well. Freezing was especially useful for preserving

Table 1. General Properties of the Amino Acids Used as DTC Precursors in This Study

	glycine	lysine	cysteine	aspartic acid	histidine
side chain	−H	$-(CH_2)_4NH_2$	$-CH_2SH$	$-CH_2COOH$	$-CH_2-C_3H_3N_2$
pK_a of the side chain		10.54	8.18	3.90	6.04
pH of the side chain		basic	acidic	acidic	weakly basic
solubility in water (g/100 mL H_2O at 25°C)	24.99	very soluble	very soluble	0.778	4.19

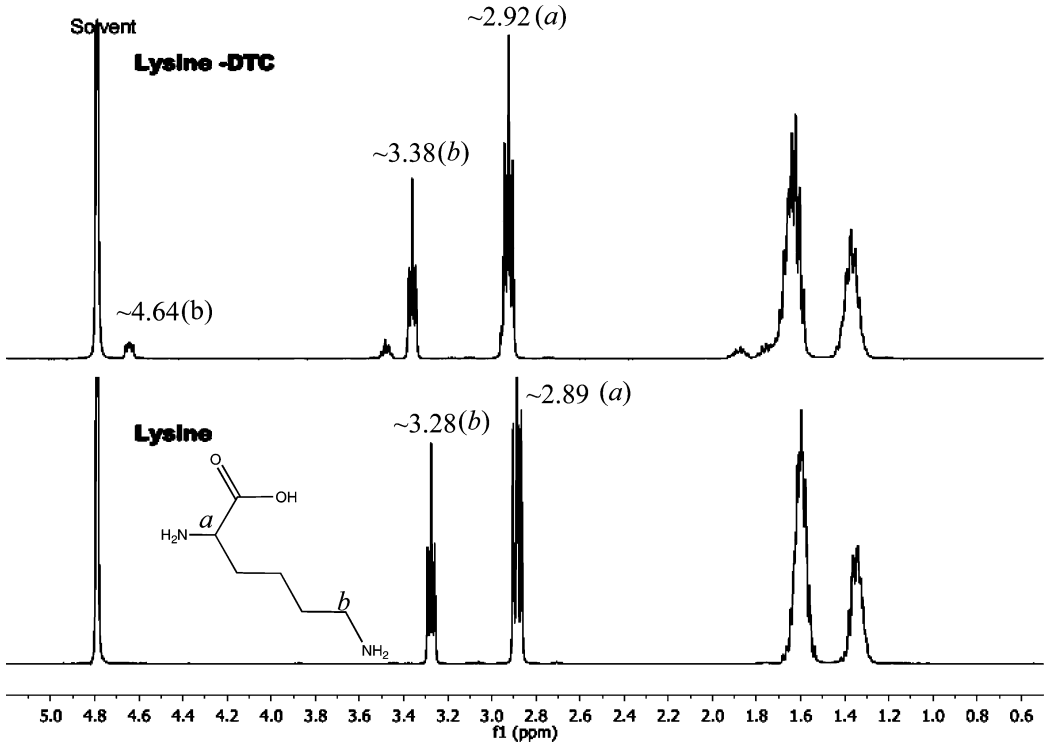

FIGURE 5. ^{1}H NMR spectra of lysine and DTC-lysine. Protons *a* and *b* show slight shifts after DTC-modification.

the properties of samples that otherwise degraded quickly when stored in the refrigerator at 4 °C. Because the shelf life of biocompatible QD samples is a constant concern (especially among commercially-available formulations), this is an attractive feature for preserving the properties of QD samples during storage.

Although monitoring UV−vis spectra from CS_2 and subsequent DTC molecules is a standard method for monitoring the reaction, we further characterized the formation of select ligands using ^{1}H NMR spectroscopy. In particular, we looked at the reaction of CS_2 with lysine due to two primary amines residing in the main and side chains. NMR spectra (Varian VXR-400 NMR, Bruker magnet, probes, and shim supply) were obtained in D_2O solvent with results shown Figure 5. In the ^{1}H NMR spectrum of lysine, the chemical shift of protons *a* (next to the α-amine, Figure 5 inset chemical structure) and protons *b* (next to the amine in the side chain) are ~2.89 and ~3.28 ppm, respectively. Once the amines reacted with CS_2, group a shifted to ~4.64 ppm and group *b* shifted to ~3.38 ppm. As shown in Figure 5, a subset of group *a* shifted to ~4.64 ppm indicating the side chain amine is preferable over the α-amine. Similar NMR spectra are required for characterizing prospective amine-containing molecules having multiple 1° and 2° amine groups (e.g., arginine). In general, however, it is sufficient to monitor the reaction extent through UV-vis absorption alone (26).

Fluorescence Quantum Yield. A critical finding of our work showed that that quantum yield (QY) of these DTC-capped QDs can be sustained immediately following the biphasic exchange and often long afterward. With many common ligand exchange procedures (including those with monothiol acids or DHLA) there is always a significant loss of QY following the transition from organic solvents into water (the QY is usually below 0.20) (10). We hypothesize that the biphasic exchange procedure has certain advantages over prior reports of DTC ligand exchange in purely organic solvents. This may be due to the nearly simultaneous DTC reaction and ligand exchange steps where densely coated QDs are continuously and selectively transferred into the aqueous phase. As Figure 1 shows, upon inspection, the qualitative brightness of the organic layer (bottom) is similar to that of aqueous layer (top), suggesting a similar QY since the QDs have identical concentrations when fully distributed in either phase. The measured fractional QY for the particular DTC-Lys QD sample in Figure 1 (594 nm emission maximum) is 0.41 as determined using a dye standard (Rhodamine 6G) compared to the initial QY of hydrophobic QDs of 0.36. This nominal gain in QY upon transfer to water is highly unusual for water-soluble ligand exchange procedures and has not been reported when using monothiols or DHLA as capping ligands. We point out, however, that not

Table 2. Quantum Yield[a] Data for Various QD Samples

λ_{max} (nm)	toluene	$CHCl_3$ (1×)[b]	$CHCl_3$ (3×)[c]	pH 8 buffer (Cys)[d]	1× PBS (Lys)[e]
509	0.58			0.45	
594	0.36				0.41
600	0.40	0.31	0.28		0.47
612	0.34	0.31	0.30	0.16	0.18
616	0.23	0.22	0.18		0.16

[a] Quantum yields determined against dye standards: fluorescein in 0.1 M NaOH (509 sample) and Rhodamine 6G in ethanol (594, 612, 600, and 616 samples). [b] Precipitated from toluene with dry methanol once and resuspended in chloroform. [c] Precipitated from toluene with dry methanol three times and resuspended in chloroform. [d] DTC-Cys capped QD suspended in pH 8 buffer. [e] DTC-Lys capped QD suspended in 1× PBS (pH 7.4).

every biphasic exchange procedure results in the preservation or increase of QY between phases. Depending on the specific conditions used and the initial quality of the QDs, the ultimate QY in water may drop well below the initial QY in the organic phase and appears to vary considerably from batch to batch. Table 2 summarizes QY measurements made before and after DTC ligand exchange using a suitable dye standard (fluorescein or Rhodamine 6G). To ensure successful biphasic exchange and to maximize QY, the inorganic synthesis procedure (precursors, temperature, injection time, polydispersity, etc.) of CdSe-ZnS QDs requires careful consideration. The final QY of DTC-capped QDs appears to be largely dependent on the quality of CdSe core and the integrity of the ZnS shell. Because many prior reports have examined DTC capping of CdSe QDs, there is less data available for QDs having ZnS shell layers. We have found that QDs with several annealed (three or more) ZnS layers appear to be more receptive to this processing step than QDs with relatively thin shells. Overall, the QY of DTC-capped QDs invariably exceeds that of DHLA-capped QDs when the same hydrophobic CdSe-ZnS nanocrystals are processed in parallel.

Ligand Density. Since the density of capping ligands is intimately related to colloidal stability and surface passivation effects (i.e. quantum yield), we estimated the DTC ligand coverage of these hydrophilic QDs. Following biphasic exchange, the newly water-soluble QDs were purified using a suitable centrifugal membrane filter (50 kDa MW cutoff or smaller) as described previously where the aqueous solution passing through the filter was collected and freeze-dried. The dry sample, solely consisting of excess ligands that were not bound to the nanocrystal surface, was weighed with a precise analytical balance. With the weight of reacted precursor known (in cases where the reaction conversion was near 100% as determined spectroscopically), the coverage of QDs was deduced to be ~800−1000 DTC-ligand molecules per QD (having a mean estimated surface area of $\sim 1.6 \times 10^4$ Å^2 per nanocrystal assuming QDs to be perfect spheres). This ligand density compares favorably to estimates with DHLA-capped QDs and suggests that DTC-ligands have superior affinity for the ZnS shell than DHLA. Further, the estimated DTC ligand density (~18 Å^2/molecule) implies that there is efficient molecular packing through self-assembly on the nanocrystal surface, especially relative to densities achieved with DHLA. Although there are several possible methods for estimating the ligand density (e.g., electrophoresis, NMR, FRET, etc.), the mass-based procedure is likely the most accurate because it is a direct measurement of material and does not require a control sample or calibration curve. Sources of measurement error include the surface area distribution of the QDs and the potential for DTC ligands to bind the filter or container surface. Because larger red-emitting CdSe-ZnS QDs and multiple ZnS layers tend to be more prolate ellipsoidal in shape (6, 37), it is likely that the effective mean surface area is larger than the estimates based on the assumption of a perfectly spherical population of nanocrystals. This suggests that the density is likely lower than our calculated estimates; however, a more precise estimate would require a thorough examination of the nanocrystal shapes using a method like transmission electron microscopy (TEM). Further, the inferred number of DTC ligands bound per QD is perhaps overestimated based on the assumption that any material not collected and weighed must be present on the QDs. While it is difficult to gauge the uncertainty in the ligand density estimate, the calculated value is reasonable based on the geometry of the nanocrystal and the minimum estimated occupied area of the QD-bound DTC molecule. The presence of even a few hundred DTC ligands per QD suggests an efficient cap exchange procedure. We assert that ligand density correlates strongly with long-term colloidal stability and preservation of photoluminescence, however this is not a function of the ligand alone. In our experience, the integrity and quality of the outermost shell layer (in this case, ZnS) is paramount to realizing high quality water-soluble QDs. This is encouraged by the slow growth and annealing of several ZnS monolayers on the CdSe core. In some cases, DTC ligands that typically produce high-QY water-soluble CdSe-ZnS confer poor luminescence, and most evidence implicates poor inorganic synthetic conditions. Furthermore, there appear to be inherent advantages the biphasic reaction and exchange process, which usually leads to a high ligand density.

Accessibility of the Nanocrystal Surface. Water-soluble QDs are unique donor fluorophores in FRET-based applications (38−41) and are especially appealing for biosensing assays. Due to their large surface area-to-volume ratio, QDs can bind multiple His-tagged peptides or proteins through metal-affinity coordination (22). This increased avidity has already been shown to substantially improve the effective FRET efficiency per QD. A notable distinguishing feature of water-soluble QDs prepared by ligand displacement versus many commercially available samples is the effective thickness of the ligand coating. Commercially prepared QDs often use bulky amphiphilic capping ligands (e.g., phospholipids or synthetic polymers), which limit their suitability for most FRET applications (42). More compact ligands allow direct binding and accessibility to the QD surface thereby improving energy transfer. Because the FRET efficiency is a strong function of the fluorescence QY and donor−acceptor center-to-center separation distance, an ideal QD would be highly luminescent with a low-molecular-weight capping ligand used to suppress non-radiative decay of the exciton and promote compatibility with solution. Due to the high coverage of DTC-capped QDs assessed previously, one concern is that His-tagged peptides and proteins may not sufficiently bind to the surface of these QDs due to limited access to the nanocrystal outer surface. However, panels b and d in Figure 6 show favorable interaction of the DTC-Lys QDs with AlexaFluor (AF) 647-labeled peptides (H_6-G_8-FTPESLRAGC, synthesized by the Iowa State Protein Facility) as well as Cy3-labeled Sec9 proteins (43), both having terminal His-tags. As a comparison, corresponding self-assembly titration data of DHLA-capped QDs with

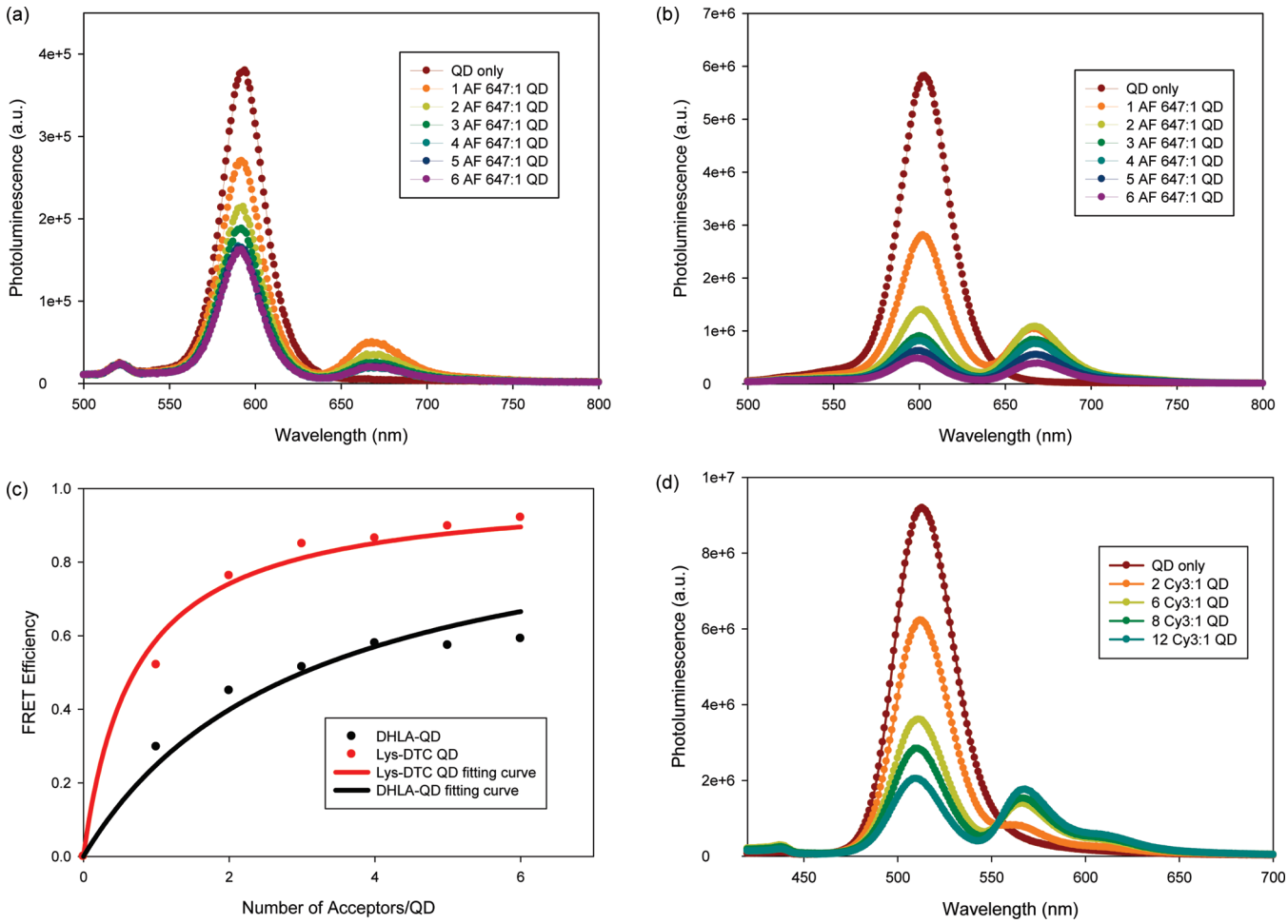

FIGURE 6. (a) Fluorescence spectra of increasing Cy5-labeled His-tagged peptide added to DHLA-coated QDs. (b) Fluorescence spectra of increasing Cy5-labeled His-tagged peptide added to DTC-Lys QDs. (c) FRET efficiency versus the number of AF 647 per QD. (d) Fluorescence spectra of increasing Cy3-labeled His-tagged proteins added to DTC-Lys QDs. The QD signal quenches rapidly suggesting a high binding affinity.

AF647-labeled His-tagged peptides (Figure 6a) are also shown. All the spectra shown in Figure 6 had the background fluorescence signal (due to direct excitation) of the dyes subtracted. In panels a and b in Figure 6, the concentration of QDs was identical and was prepared from same initial stock of hydrophobic QDs. As is immediately evident, the QY of DTC-Lys QDs is about 15-fold higher than that of DHLA-capped QDs based on the measured fluorescence signal of each sample. Figure 6b also shows direct evidence of QDs having high QY where the loss of integrated QD emission intensity is several fold larger than the integrated enhanced emission of AF647 dye. This is due to a pronounced difference between the donor and acceptor QY. In prior QD-based FRET studies, the QD and dye have often had similar QY (around 0.15) and therefore exhibited similar changes in integrated fluorescence signal during a titration experiment (41). To show the further benefit of these DTC-capped QDs, a comparison of FRET efficiency between DTC-Lys QDs and DHLA-capped QDs is shown in Figure 6c. The experimental data is fitted by a modified Förster model that accounts for multiple acceptors (41). Obviously, the FRET efficiency of DTC-Lys QDs is significantly higher than that of DHLA-capped QDs because of their much higher quantum yield with the assumption that the donor–acceptor distances are similar for the two QD formulations. These DTC-capped QDs not only have desirably thin coatings to minimize the FRET donor–acceptor distance and limit steric interference with binding, but also have high fluorescence QY, which leads to improved FRET efficiency.

pH Sensitivity of Cap-Exchanged QDs. One major drawback of DHLA-capped QDs (and related monothiol alkyl carboxyl species) is their irreversible and spontaneous precipitation in acidic media. This is perhaps one of the most significant limitations to the use of DHLA as a compact biocompatible ligand and is well-documented in the literature (44). By contrast, we have found that the pH sensitivity of DTC-capped QDs is readily modified by altering the specific functional groups expressed on the ligand. As an example, the photoluminescence (PL) of DTC-Lys QDs dropped only slightly as the pH decreased from 7 (neutral) to 6 (slightly acidic) and was surprisingly stable in buffered solutions ranging from pH 4 to 6 (Figure 7a). By adding aspartic acid (Asp) as a secondary capping ligand, the PL stability in acidic solutions improved considerably as shown in Figure 7b. We attribute this behavior to the relatively low pK_a of the side chain on Asp. For comparison, the same pH sensitivity study was conducted using DHLA-capped QDs. We found that DHLA-

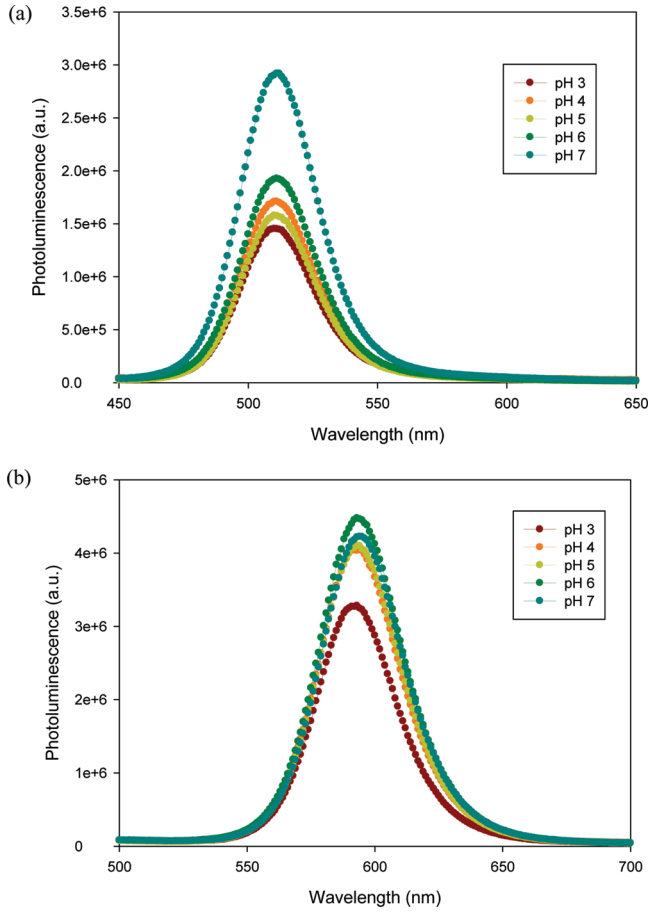

FIGURE 7. (a) Measured fluorescence spectra of DTC-Lys QDs in pH 3−7 buffer solutions. (b) Measured fluorescence spectra of DTC-Lys-Asp QDs in pH 3−7 buffer solutions.

capped QDs immediately precipitated once the pH dropped below 7 as expected (Figure 8a), whereas DTC-Lys QDs were stable (showing no visible precipitation) over a wide range of acidic buffer solutions (pH 4−7) for many days, as shown in Figure 8b−d. Although many other QD formulations have proved stable in acidic conditions, most of these require relatively thick coatings to isolate the embedded nanocrystal from solution. An advantage of the present method is the ability to confer a wide range of pH stability with a monolayer of low-molecular-weight ligands.

An interesting if unexpected finding in the study of pH sensitivity is that DTC-cysteine (Cys) QDs effectively functioned as reversible luminescent pH sensors. We observed that the PL dropped dramatically as the pH was lowered (Figure 9a); however, the PL was partially recovered by adding a strong base (such as sodium hydroxide, NaOH, at an appropriate concentration) as shown in Figure 9b, where the recovery improved steadily over time. Although the PL dropped substantially once the pH was lowered below 6, no visible precipitation was observed during the experiment as shown in Figure 10. This sharply contrasts the immediate coagulation and loss of PL characteristic of DHLA-capped QDs in acidic media. These results suggest that the process by which DTC-Cys QDs lose their PL in acidic media is inherently different from that of DHLA-capped QDs.

The mechanism by which DTC-Cys QDs exhibit pH sensitivity with reversible PL loss is believed to be influenced by formation of disulfide bonds between Cys ligands on neighboring QDs. This bridging interaction brings many DTC-Cys QDs into near contact sufficient to induce fluorescence self-quenching. The disulfide bond is easily broken with the addition of a strong base or reducing agent which disrupts QD aggregates and significantly restores the PL close to its original level. We have carried out several experiments to support this observation. As shown in Figure 11, rather than using a single population of QDs, two independent populations of QDs (having emission maxima centered at 509 nm and 599 nm, respectively) were mixed in specific molar ratios. The equimolar mixture of DTC-Cys QD509 and DTC-Cys QD599 (1:1 ratio) shows that the former QD fluorescence is almost completely quenched at pH 3, whereas the latter shows a small but appreciable PL signal. If we compare this result with the control sample of DTC-Cys QD599 at pH 3 (where the QD599 concentration is held constant throughout), there is a slight enhancement of the QD599 signal in the mixed

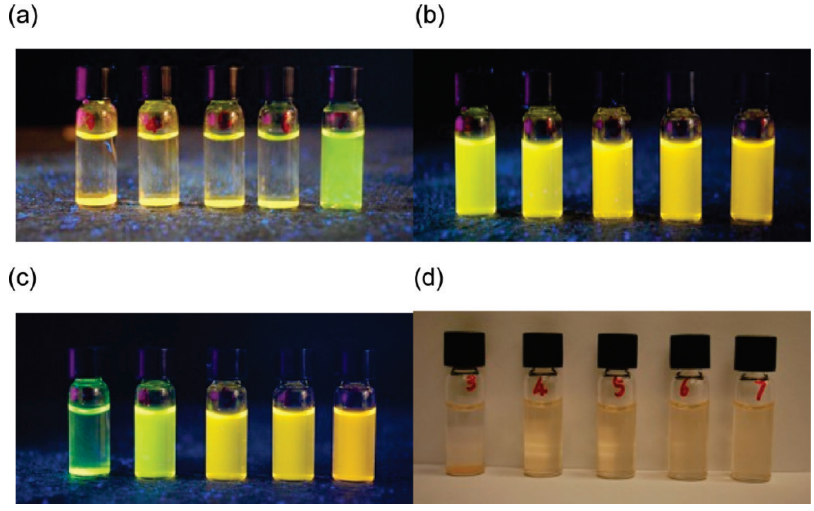

FIGURE 8. (a) DHLA-coated QDs in pH 3−7 buffer solutions (left to right) under UV light. (b) DTC-Lys QDs in pH 3−7 buffer solutions under UV light. (c) DTC-Lys QDs in pH 3−7 buffer solutions after 5 days under UV light. (d) DTC-Lys QDs in pH 3−7 buffer solutions after 5 days under ambient light.

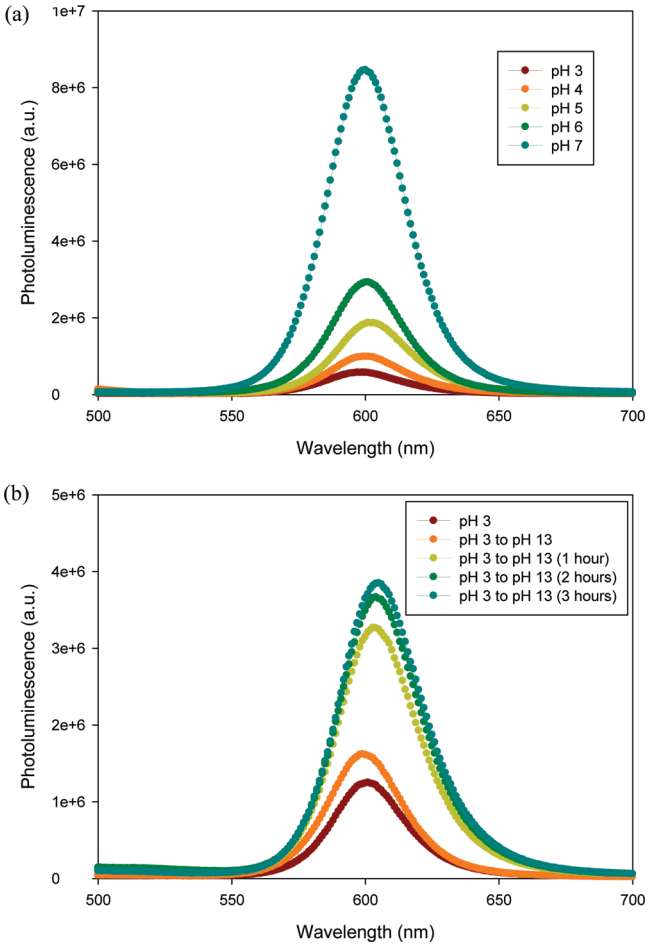

FIGURE 9. (a) Measured fluorescence spectra of DTC-Cys QDs in pH 3−7 buffer solutions. (b) Measured fluorescence spectra of DTC-Cys QDs in pH 3, and the same samples measured after being basified to pH 13 at various time periods (0−3 h).

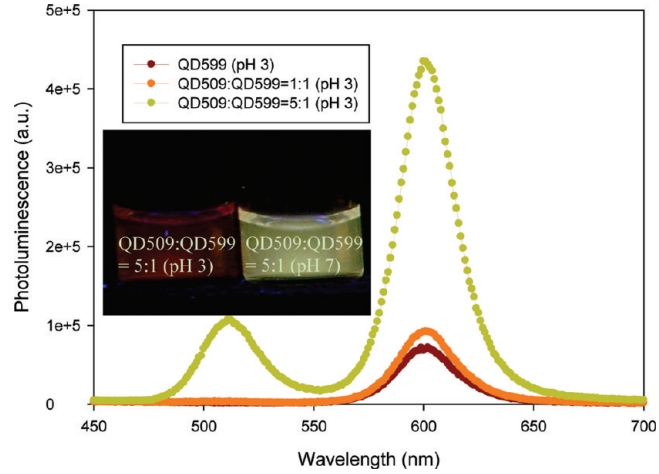

FIGURE 11. Measured fluorescence spectra of QD599 and QD509-QD599 mixtures in pH 3 buffer solutions. The inset shows an image of the 5:1 ratio mixture at pH 3 and 7 and excited with a UV lamp (λ_{ex} = 365 nm). The fluorescence color change is consistent with the measured spectra.

sample. This result suggests the possibility that the QD599 population is receiving energy from the QD509 population where there is sufficient contact between QDs (45). This interaction is further clarified by increasing the ratio of QD509 in the mixed sample to 5:1. In this scenario, the likelihood of QD599 (acceptor) interacting with QD509 (donor) is greatly increased. We likewise see a dramatic increase in the QD599 signal consistent with our hypothesis that there is energy transfer occurring between these distinct populations facilitated by specific binding interactions occurring between them. The inset image in Figure 10 shows a substantial change in emission color with pH (near white at pH 7 to red at pH 3).

Although we can infer some association of QDs at low pH due to fluorescence self-quenching, this behavior appeared to be insufficient for widespread precipitation and loss of solubility in water. Throughout the cycling of pH between basic and acidic conditions, the Cys-capped QDs appeared to be fully soluble (i.e., forming transparent solutions) and free of large aggregates. To determine the origin of this binding interaction, we used dithiothreitol (DTT), a common reducing agent, to test whether fluorescence quenching was due, at least in part, to disulfide bridging between neighboring QDs. During the experiment, DTC-Cys QDs in pH 3 buffer was basified to pH 7 before adding DTT (the reduction via DTT is most effective in basic conditions). As Figure 12 shows, DTC-Cys QDs in acidic buffer showed a modest PL increase when the pH was returned to 7 after 2 h; however, the addition of DTT was critical to restoring most of the PL to the original level in neutral buffer. The significant PL recovery achieved by adding a reducing agent at pH 7 suggests that the association between QDs was largely due to reversible disulfide bridging interactions.

Potential of DTC-Capped QDs in Cell Studies. A desirable application of water-soluble QDs is for biological studies and especially experiments using living cells or tissue samples (3, 46). To test the performance of QDs capped with DTC-based ligands, we introduced these nanocrystals into the growth media of MDA-MB-231 breast cancer cells adhered to collagen-coated glass coverslips and imaged the cells using total internal refection fluorescence (TIRF) microscopy. While some QDs were observed to nonspecifically bind to the collagen surface, most nanocrystals that remain following washing are bound to the surface of cells or were

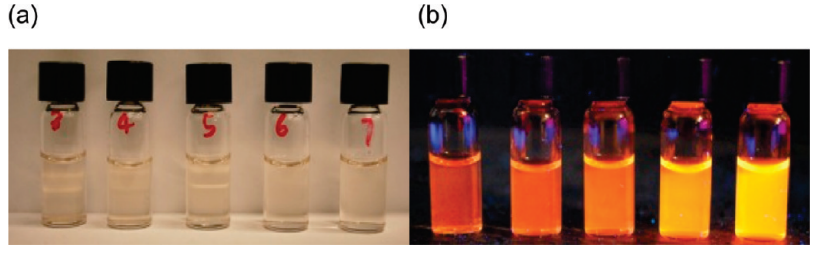

FIGURE 10. (a) DTC-Cys QDs in pH 3−7 buffer solutions under normal light. (b) DTC-Cys QDs in pH 3 to 7 buffer solutions under UV light.

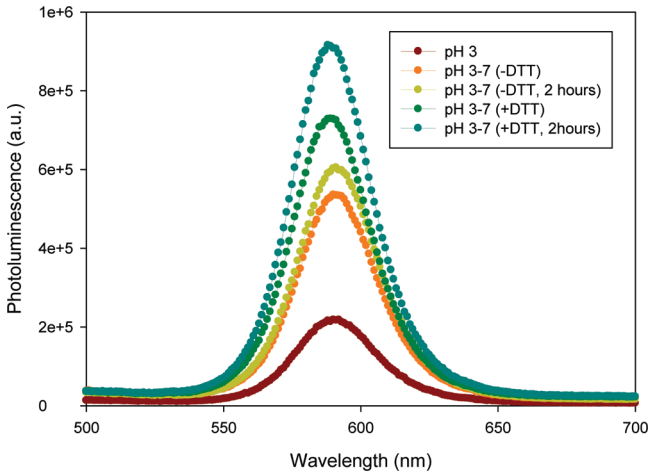

FIGURE 12. Measured fluorescence spectra of DTC-Cys QDs in pH 3 solution and after being basified to pH 7.

internalized within cells through endo- or pinocytosis (Figure 13). The TIRF system allowed us to change the illumination penetration depth continuously from ~100 nm to full epi-illumination. Limiting the illumination depth improves fluorescence contrast and lowers the background signal. Time-lapse imaging showed that QDs preserved their luminescence properties over the duration of the incubation and imaging (hours to days). The cells showed no obvious signs of nanoparticle toxicity (Figure 13c) during any phase of the experiments, which is consistent with previous studies (47) using water-soluble CdSe-ZnS QDs having a variety of hydrophilic surface coatings. Of note is the ability to follow QD fluorescence for long periods of time and through long exposure to the TIRF illumination source. Photobleaching is a common limitation of traditional dye labels, however the DTC-capped QDs did not suffer noticeable loss of luminescence over the duration of imaging (on the order of a few hours). The labeling in this study was effectively non-specific, however one tantalizing aspect of the DTC ligand exchange procedure is the potential for targeting water-soluble QDs to specific regions of the cell (interior or exterior) for long-term imaging and biosensing. This goal may be realized by coupling unique DTC ligands with His-tagged biomolecules or by attaching ligands and biomolecules using DTC derivatives. The prospect of using DTC as the anchoring group to QDs is attractive in that it avoids variability between methods (e.g., His-tagged versus DTC affinity) and streamlines the process of creating customized QDs for biological applications. Custom synthetic peptides are particularly well-suited for DTC modification of a unique Cys residue that affords affinity for the nanocrystal surface. Proteins could also be attached in this manner but may require substantially more effort in certain cases. We are currently investigating the feasibility of this approach and will report on progress in a future publication.

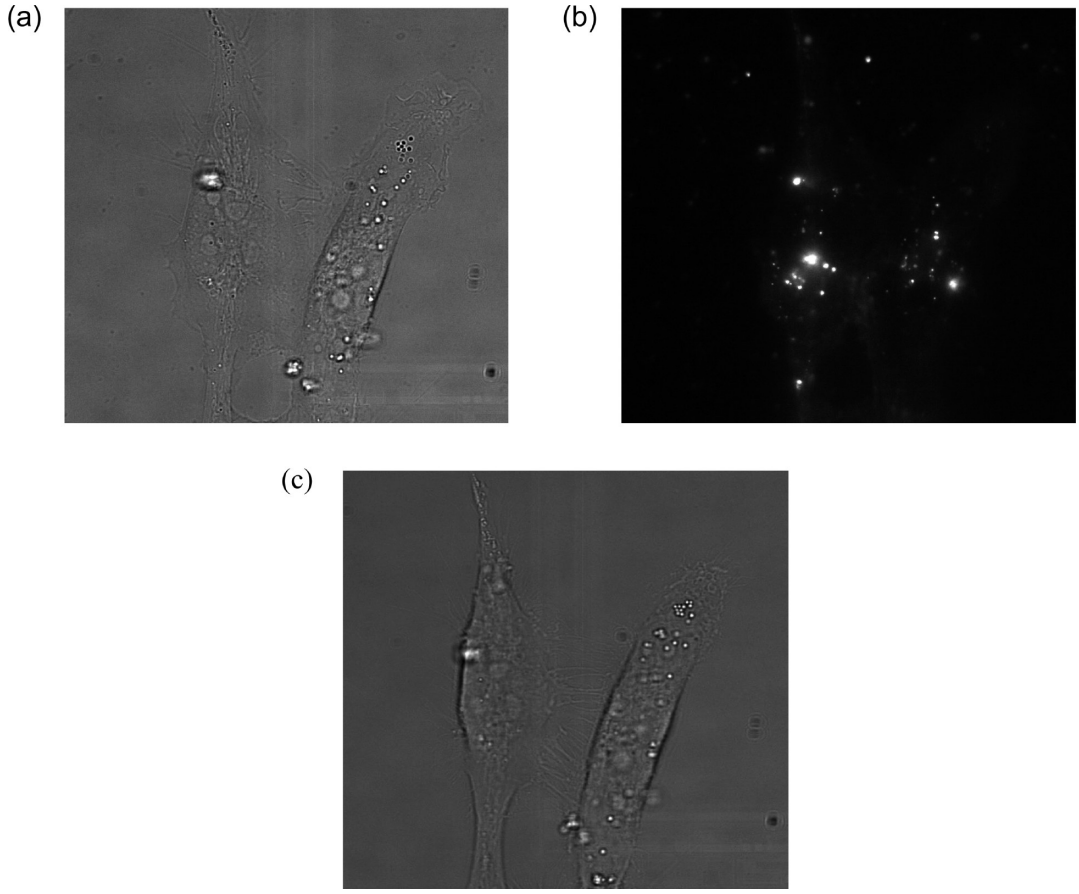

FIGURE 13. (a) Bright-field image of untreated MDA-MB-231 cells. (b) Fluorescence image of DTC-Cys QDs labeled MDA-MB-231 cells using total internal reflection fluorescence (TIRF) microscopy. (c) Bright-field image of MDA-MB-231 cells after QD labeling and exposure to the TIRF laser (λ_{em} = 442 nm) for 30 min.

CONCLUSIONS

We have investigated the performance and behavior of dithiocarbamate ligands to render hydrophobic CdSe-ZnS QDs water-soluble through a single step reaction and cap exchange procedure. Specifically, we explored pH sensitivity, ability to function in FRET-based experiments, and compatibility in cell-based biological studies of these newly produced water-soluble QDs. DTC ligands bind more stably to the semiconductor shell than other thiolated molecules and can maintain a high quantum yield relative to native hydrophobic QDs capped with alkyl phosphines. The relatively high density of ligands occupying the QD surface is important for colloidal stability yet still allows His-tagged biomolecules to bind the QD surface directly. In general, the FRET efficiency using DTC-capped QDs improves substantially due to the higher fluorescence quantum yield of optimally prepared samples. These QDs were also shown to be appropriate for cell labeling studies where fluorescence was sustained over several hours and no obvious toxicity effects were observed. Compared to DHLA-capped QDs (and related functionalized derivatives) which have a more cumbersome reaction and ligand exchange process, DTC chemistry is a facile method that leads to hydrophilic QDs with high quantum yield. The success of this approach for CdSe-ZnS is thought to be a function of the DTC ligand molecules, quality of the synthesized nanocrystals, and biphasic exchange process which when optimized lead to dense coverage of ligands on the QD surface. By using different amino precursors, the pH sensitivity and other behavior can be carefully controlled, which is appealing for future biomedical applications using these QDs.

Acknowledgment. We acknowledge financial support from startup funds at Iowa State University, Dr. Yeon-Kyun Shin (Iowa State, Department of Biochemistry, Biophysics & Molecular Biology) for kindly supplying dye-labeled proteins, Dr. Ian Schneider (Iowa State, Chemical & Biological Engineering) for providing cell culturing and imaging support, and Joel Nott of the Iowa State Protein Facility for assistance with peptide synthesis.

REFERENCES AND NOTES

(1) Medintz, I. L.; Mattoussi, H.; Clapp, A. R. *Int. J. Nanomed.* **2008**, *3*, 151–167.
(2) Xing, Y.; Rao, J. *Cancer Biomarkers* **2008**, *4*, 307–319.
(3) Michalet, X.; Pinaud, F. F.; Bentolila, L. A.; Tsay, J. M.; Doose, S.; Li, J. J.; Sundaresan, G.; Wu, A. M.; Gambhir, S. S.; Weiss, S. *Science* **2005**, *307*, 538–544.
(4) Robel, I.; Subramanian, V.; Kuno, M.; Kamat, P. V. *J. Am. Chem. Soc.* **2006**, *128*, 2385–2393.
(5) McDonald, S. A.; Konstantatos, G.; Zhang, S.; Cyr, P. W.; Klem, E. J. D.; Levina, L.; Sargent, E. H. *Nat. Mater.* **2005**, *4*, 138–142.
(6) Dabbousi, B. O.; Rodriguez-Viejo, J.; Mikulec, F. V.; Heine, J. R.; Mattoussi, H.; Ober, R.; Jensen, K. F.; Bawendi, M. G. *J. Phys. Chem. B* **1997**, *101*, 9463–9475.
(7) Cordero, S. R.; Carson, P. J.; Estabrook, R. A.; Strouse, G. F.; Buratto, S. K. *J. Phys. Chem. B* **2000**, *104*, 12137–12142.
(8) Wang, Q.; Xu, Y.; Zhao, X.; Chang, Y.; Liu, Y.; Jiang, L.; Sharma, J.; Seo, D.; Yan, H. *J. Am. Chem. Soc.* **2007**, *129*, 6380–6381.
(9) Mattoussi, H.; Mauro, J. M.; Goldman, E. R.; Anderson, G. P.; Sundar, V. C.; Mikulec, F. V.; Bawendi, M. G. *J. Am. Chem. Soc.* **2000**, *122*, 12142–12150.
(10) Gao, X.; Cui, Y.; Levenson, R. M.; Chung, L. W. K.; Nie, S. *Nat. Biotechnol.* **2004**, *22*, 969–976.
(11) Bruchez, M.; Moronne, M.; Gin, P.; Weiss, S.; Alivisatos, A. P. *Science* **1998**, *281*, 2013–2016.
(12) Gerion, D.; Pinaud, F.; Williams, S. C.; Parak, W. J.; Zanchet, D.; Weiss, S.; Alivisatos, A. P. *J. Phys. Chem. B* **2001**, *105*, 8861–8871.
(13) Dubertret, B.; Skourides, P.; Norris, D. J.; Noireaux, V.; Brivanlou, A. H.; Libchaber, A. *Science* **2002**, *298*, 1759–1762.
(14) Chan, W. C. W.; Nie, S. *Science* **1998**, *281*, 2016–2018.
(15) Oh, J. K. *J. Mater. Chem.* **2010**, *20*, 8433.
(16) Pathak, S.; Choi, S.; Arnheim, N.; Thompson, M. E. *J. Am. Chem. Soc.* **2001**, *123*, 4103–4104.
(17) Mattoussi, H.; Mauro, J.; Goldman, E.; Green, T.; Anderson, G.; Sundar, V.; Bawendi, M. *Phys. Status Solidi B* **2001**, *224*, 277–283.
(18) Aldana, J.; Wang, Y. A.; Peng, X. *J. Am. Chem. Soc.* **2001**, *123*, 8844–8850.
(19) Hanaki, K.; Momo, A.; Oku, T.; Komoto, A.; Maenosono, S.; Yamaguchi, Y.; Yamamoto, K. *Biochem. Biophys. Res. Commun.* **2003**, *302*, 496–501.
(20) Koneswaran, M.; Narayanaswamy, R. *Sens. Actuators, B* **2009**, *139*, 91–96.
(21) Pong, B.; Trout, B. L.; Lee, J. *Langmuir* **2008**, *24*, 5270–5276.
(22) Medintz, I. L.; Uyeda, H. T.; Goldman, E. R.; Mattoussi, H. *Nat. Mater.* **2005**, *4*, 435–446.
(23) Chan, W. C. W.; Maxwell, D. J.; Gao, X.; Bailey, R. E.; Han, M.; Nie, S. *Curr. Opin. Biotechnol.* **2002**, *13*, 40–46.
(24) Uyeda, H. T.; Medintz, I. L.; Jaiswal, J. K.; Simon, S. M.; Mattoussi, H. *J. Am. Chem. Soc.* **2005**, *127*, 3870–3878.
(25) Mei, B. C.; Susumu, K.; Medintz, I. L.; Mattoussi, H. *Nat. Protoc.* **2009**, *4*, 412–423.
(26) Zhu, H.; Coleman, D. M.; Dehen, C. J.; Geisler, I. M.; Zemlyanov, D.; Chmielewski, J.; Simpson, G. J.; Wei, A. *Langmuir* **2008**, *24*, 8660–8666.
(27) Zhao, Y.; Pérez-Segarra, W.; Shi, Q.; Wei, A. *J. Am. Chem. Soc.* **2005**, *127*, 7328–7329.
(28) Querner, C.; Reiss, P.; Bleuse, J.; Pron, A. *J. Am. Chem. Soc.* **2004**, *126*, 11574–11582.
(29) von Wrochem, F.; Gao, D.; Scholz, F.; Nothofer, H.; Nelles, G.; Wessels, J. M. *Nat. Nano* **2010**, *5*, 618–624.
(30) Wang, J.; Xu, J.; Goodman, M. D.; Chen, Y.; Cai, M.; Shinar, J.; Lin, Z. *J. Mater. Chem.* **2008**, *18*, 3270–3274.
(31) Dubois, F.; Mahler, B.; Dubertret, B.; Doris, E.; Mioskowski, C. *J. Am. Chem. Soc.* **2007**, *129*, 482–483.
(32) Querner, C.; Benedetto, A.; Demadrille, R.; Rannou, P.; Reiss, P. *Chem. Mater.* **2006**, *18*, 4817–4826.
(33) Clapp, A. R.; Goldman, E. R.; Mattoussi, H. *Nat. Protoc.* **2006**, *1*, 1258–1266.
(34) Howarth, M.; Liu, W.; Puthenveetil, S.; Zheng, Y.; Marshall, L. F.; Schmidt, M. M.; Wittrup, K. D.; Bawendi, M. G.; Ting, A. Y. *Nat. Methods* **2008**, *5*, 397–399.
(35) Budavari, S.; O'Neil, M.; Smith, A.; Heckelman, P.; Obenchain, J. *The Merck Index*, 12th ed.; CRC Press: Boca Raton, FL, 1996.
(36) Weast, R. C. *CRC Handbook of Chemistry and Physics*; CRC Press: Boca Raton, FL, 1977.
(37) Manna, L.; Wang; Cingolani, R.; Alivisatos, A. P. *J. Phys. Chem. B* **2005**, *109*, 6183–6192.
(38) Willard, D. M.; Carillo, L. L.; Jung, J.; Van Orden, A. *Nano Lett.* **2001**, *1*, 469–474.
(39) Suzuki, M.; Husimi, Y.; Komatsu, H.; Suzuki, K.; Douglas, K. T. *J. Am. Chem. Soc.* **2008**, *130*, 5720–5725.
(40) Mattoussi, H.; Medintz, I.; Clapp, A.; Goldman, E.; Jaiswal, J.; Simon, S.; Mauro, J. *J. Assoc. Lab. Autom.* **2004**, *9*, 28–32.
(41) Clapp, A. R.; Medintz, I. L.; Mauro, J. M.; Fisher, B. R.; Bawendi, M. G.; Mattoussi, H. *J. Am. Chem. Soc.* **2004**, *126*, 301–310.
(42) Pons, T.; Uyeda, H. T.; Medintz, I. L.; Mattoussi, H. *J. Phys. Chem. B* **2006**, *110*, 20308–20316.
(43) Su, Z.; Ishitsuka, Y.; Ha, T.; Shin, Y. *Structure* **2008**, *16*, 1138–1146.
(44) Susumu, K.; Uyeda, H. T.; Medintz, I. L.; Pons, T.; Delehanty, J. B.; Mattoussi, H. *J. Am. Chem. Soc.* **2007**, *129*, 13987–13996.
(45) Somers, R. C.; Bawendi, M. G.; Nocera, D. G. *Chem. Soc. Rev.* **2007**, *36*, 579–591.
(46) Derfus, A. M.; Chan, W.; Bhatia, S. *Adv. Mater.* **2004**, *16*, 961–966.
(47) Jaiswal, J. K.; Simon, S. M. *Trends Cell Biol.* **2004**, *14*, 497–504.

AM100996G